

A new limit on Lorentz-violating tensor interactions set using ^{21}Ne -Rb-K comagnetometer

M. Smiciklas, J. M. Brown, L.W. Cheuk, and M. V. Romalis
Department of Physics, Princeton University, Princeton, New Jersey 08544

We develop a comagnetometer using ^{21}Ne atoms with nuclear spin $I = 3/2$ and Rb atoms polarized by spin-exchange with K atoms to search for tensor interactions that violate local Lorentz invariance. We frequently reverse orientation of the experiment and search for signals at the first and second harmonics of the sidereal frequency. We constrain 4 of the 5 spatial Lorentz-violating coefficients c_{jk}^n that parameterize variations in the maximum attainable speed of a neutron at a level of 10^{-29} , improving previous limits by 2 to 4 orders of magnitude and placing the most stringent limit on tensor Lorentz violation for a fermion.

PACS numbers: 11.30.Cp, 11.30.Er, 21.30.Cb, 32.30.Dx

Searches for coupling of a nuclear quadrupole moment to a possible spatial anisotropy were first performed by Hughes [1] and Drever [2] using ^7Li NMR and have since been improved with ^7Be [3], ^{201}Hg [4], and ^{21}Ne [5] nuclei. They have been interpreted as the most stringent tests of local Lorentz invariance within the $TH\epsilon\mu$ formalism [6] that describes deviations from the Einstein Equivalence Principle [7]. More recently, these experiments have been used to constrain CPT-even Lorentz-violating parameters within the Standard Model Extension (SME) developed by Kostelecký [8, 9]. Due to a finite kinetic energy of valence nucleons, tensor NMR energy shifts are sensitive to possible variation in the maximum attainable particle velocity [7, 10] and can be directly compared to the limits on Lorentz violation from ultra-high energy cosmic rays and other astrophysical phenomena [11–13]. It can be argued that Lorentz invariance is likely to be broken at some level by the effects of quantum gravity which contains a dimensionfull Planck scale that is not Lorentz-invariant. Popular ideas for quantum gravity theories, such as the Hořava-Lifshitz model [14], explicitly violate Lorentz symmetry. CPT-even Lorentz violation is particularly interesting to explore because it is not as well constrained as CPT-odd effects and does not suffer from the associated fine-tuning problems [15, 16].

Here we describe a new comagnetometer developed to search for Lorentz-violating tensor interactions. It is based on the K- ^3He comagnetometer, previously used to constrain Lorentz-violating vector spin interactions [17]. The ^3He is replaced by ^{21}Ne with nuclear spin $I = 3/2$. Since the gyromagnetic ratio of ^{21}Ne is about an order of magnitude smaller than that of ^3He , the comagnetometer has an order of magnitude better energy resolution for the same level of magnetic field sensitivity. In order to overcome a faster nuclear spin relaxation in ^{21}Ne relative to ^3He due to electric quadrupole interactions, we replace K with Rb atoms, which have a faster spin-exchange rate with ^{21}Ne [18], and increase their density. We rely on hybrid optical pumping [19], using spin-exchange with optically-pumped K to polarize the Rb atoms while avoiding strong absorption of pumping light by the optically dense Rb vapor.

The experiment is placed on a rotary platform (see Fig. 1), so its orientation can be frequently reversed to introduce a modulation of the Lorentz-violating signal. Among lab-fixed backgrounds, only the gyroscopic signal due to Earth rotation cannot be easily suppressed, and we rely on sidereal and semi-sidereal oscillations expected for Lorentz-violating effects to extract anisotropic signals of an extra-solar origin. We measure ^{21}Ne NMR frequency with sensitivity of about 0.5 nHz and within the Schmidt model for ^{21}Ne nucleus constrain 4 of the 5 spatial components of the symmetric traceless SME tensor c_{jk}^n for neutrons at a level of a few parts in 10^{-29} . This sensitivity exceeds all other laboratory limits on the $c_{\mu\nu}$ coefficients in the matter sector [20] as well as the recent limit on the neutrino c_{0j} coefficient at a level of 10^{-27} [21] and limits on c_{00} at a level of 10^{-23} from analysis of ultra-high energy cosmic rays [13, 22].

The operating principles of the comagnetometer are similar to that described in [17, 23–25]. The atoms are contained in a 1.4 cm diameter spherical cell made from aluminosilicate glass that is filled with Ne at a density of 2.03 ± 0.05 amagat, as determined from pressure broadening of Rb D1 line [26], enriched to 95% of ^{21}Ne , 30 Torr

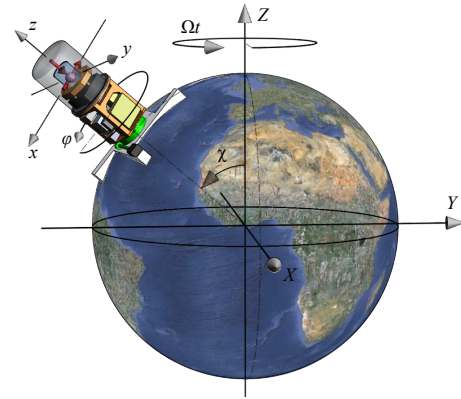


FIG. 1: The experimental apparatus is rotated around the local vertical. ^{21}Ne spins are polarized down along $-\hat{z}$ and the probe beam is directed horizontally along $-\hat{x}$

of N_2 for quenching, and a mixture of ^{87}Rb and K alkali metals. The cell is heated to about 200°C by AC currents at 170 kHz in a twisted pair wire heater. The density of Rb at the operating temperature is measured to be $5.5 \times 10^{14} \text{ cm}^{-3}$, while the density of K is about $2 \times 10^{12} \text{ cm}^{-3}$. K atoms are optically pumped by approximately 650 mW of circularly-polarized light from an amplified distributed bragg reflector diode laser at 770 nm. Rb atoms are polarized to 40% by Rb-K spin exchange collisions, while ^{21}Ne atoms are polarized to 15-17% by spin-exchange with Rb. The comagnetometer signal is measured by monitoring optical rotation of a 10 mW linearly polarized probe beam that is generated by a distributed feedback diode laser near the 795 nm Rb D1 transition. The comagnetometer cell is placed inside magnetic shields consisting of 3 layers of μ -metal and an inner ferrite shield with an overall shielding factor of 10^8 . A set of large Helmholtz coils surround the apparatus to cancel the Earth's magnetic field. Coils inside the magnetic shields are used to cancel residual magnetic fields and create a compensation field $B_z = -8\pi/3\kappa_0(M_{\text{Rb}} + M_{\text{Ne}})$, where M_{Rb} and M_{Ne} are the magnetizations of electron and nuclear spins, and $\kappa_0 = 34 \pm 3$ is the contact spin-exchange enhancement factor for Rb- ^{21}Ne [18, 27]. At this compensation field the comagnetometer signal is insensitive to slowly-changing magnetic fields in all three directions while retaining sensitivity to anomalous interactions that couple only to nuclear or electron spins. Changes in the sensitivity of the comagnetometer are periodically monitored by application of an oscillating B_x field [17]. The optical setup is contained in a bell jar evacuated to 2 Torr to eliminate noise from air currents. The apparatus and all electronics are mounted on a rotation platform and can be fully rotated around the vertical axis in several seconds.

A representative sample of the comagnetometer signal during normal data collection is shown in Fig. 2. The orientation of the platform is reversed by 180° every 22 sec. We usually collect data in the North-South (NS) orientations of the sensitive \hat{y} axis, which gives a maximum gyroscopic signal due to the Earth's rotation and in the East-West (EW) orientations, which gives nominally zero gyroscopic signal. After each mechanical rotation a background measurement of optical rotation is performed with B_z field detuned by $0.33 \mu\text{T}$ to suppress the spin response. Data collection is periodically paused (300 to 400 sec in Fig. 2) to adjust the compensation value of B_z field and calibrate the sensitivity of the magnetometer. Fig. 3 shows an example of long-term measurements of the amplitudes of NS and EW modulations after subtraction of optical rotation background. We make a 10% correction to the calibration of the comagnetometer based on the size of the gyroscopic signal due to Earth's rotation $B_{\text{eff}} = \Omega_{\oplus} \sin \chi I / \mu_{\text{Ne}} = 2.63 \text{ pT}$ in the NS data. Slow drifts in the NS and EW signals are caused by changes in various experimental parameters. We perform a correlation analysis between the comagnetometer signal and several measured temperatures, laser beam position mon-

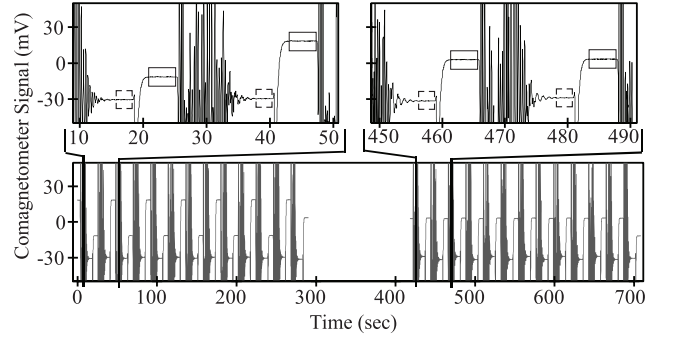


FIG. 2: Magnetometer signal as a function of time. During the first 300 seconds the \hat{y} axis is alternated between North and South directions. After the transient from rotation decays, the background optical rotation is measured (dashed box). Then B_z field is set to the compensation point and actual signal is measured (solid box). Rotations are stopped after 13 reversals for calibration. In the following sequence the \hat{y} axis is alternated between East and West.

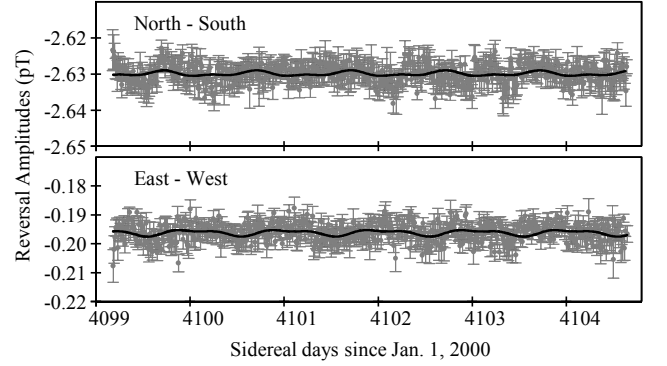


FIG. 3: Long-term measurements of the N-S and E-W modulation amplitudes with a fit including first and second harmonics of the sidereal frequency.

itors, tilts, ^{21}Ne polarization, and other parameters. We find a small but finite correlation of the signal with oven temperature, room temperature, and ^{21}Ne polarization. These correlations are removed from the data while ensuring that diurnal changes in the temperature do not accidentally cancel a real sidereal signal in the data.

We interpret these measurements within a sub-set of the SME, adding $c_{\mu\nu}$ coefficients to the standard relativistic Lagrangian of a fermion,

$$\mathcal{L} = \frac{1}{2} i \bar{\psi} (\gamma_\nu + c_{\mu\nu} \gamma^\mu) \overleftrightarrow{\partial}^\nu \psi - \bar{\psi} m \psi. \quad (1)$$

In the non-relativistic limit, this leads to an anisotropic energy shift for a particle with spatial components of momentum p_j , which can be written as a product of spherical tensor operators of rank 2, \mathcal{C}_n^2 and \mathcal{P}_n^2 , formed from Cartesian components of c_{jk} and $p_j p_k$ respectively,

$$H = -c_{jk} p_j p_k / m = -(-1)^n \mathcal{C}_n^2 \mathcal{P}_{-n}^2 / m. \quad (2)$$

Using the Wigner-Eckart theorem, we evaluate the matrix elements of \mathcal{P}_n^2 in terms of \mathcal{I}_n^2 , the rank-2 spherical tensor formed from components of nuclear spin I ,

$$\langle I, m | \mathcal{P}_n^2 | I, m' \rangle = \frac{\langle I, m | \mathcal{I}_n^2 | I, m' \rangle \langle I, I | \mathcal{P}_0^2 | I, I \rangle}{\langle I, I | \mathcal{I}_0^2 | I, I \rangle}. \quad (3)$$

In the coordinate system defined in Fig. 1, the comagnetometer is sensitive to first order to the energy of the ^{21}Ne nuclear magnetic moment μ_{Ne} interacting with the magnetic field in the \hat{y} direction [17],

$$H_B = -\mu_{\text{Ne}} I_y B_y / |I|. \quad (4)$$

Among tensor nuclear spin operators, the comagnetometer is sensitive to first order to the operator

$$H_Q = -Q(I_y I_z + I_z I_y)/2 = -iQ(\mathcal{I}_1^2 + \mathcal{I}_{-1}^2)/2, \quad (5)$$

since I_z has a finite expectation value due to longitudinal nuclear polarization of ^{21}Ne . We are sensitive to the $i(\mathcal{C}_1^2 + \mathcal{C}_{-1}^2)$ combination of the spherical tensor components of the c_{jk} coefficients in the frame of the experiment. Transforming the spherical tensor into the geocentric equatorial coordinate system, we obtain expressions for the NS and EW signals as a function of time,

$$\begin{aligned} S_{\text{NS}} &= -c'_Y \cos 2\chi \cos \Omega_\oplus t - c'_X \cos 2\chi \sin \Omega_\oplus t - \\ &\quad (c'_Z \sin 2\chi \cos 2\Omega_\oplus t + c'_- \sin 2\chi \cos 2\Omega_\oplus t)/2 \\ S_{\text{EW}} &= c'_X \cos \chi \cos \Omega_\oplus t - c'_Y \cos \chi \sin \Omega_\oplus t + \\ &\quad c'_Z \sin \chi \cos 2\Omega_\oplus t - c'_- \sin \chi \sin 2\Omega_\oplus t, \end{aligned} \quad (6)$$

where the c parameters are defined in Table 1 [20], $\chi = 49.6^\circ$ in Princeton, and t is the local sidereal time. Primes on c coefficients indicate that they are measured experimentally in magnetic field units. The signal contains both first and second harmonics of the Earth rotation rate Ω_\oplus . Each component of the c tensor can be determined independently from NS and EW signals, although sensitivity to the first harmonic in the NS data is suppressed because $\cos 2\chi = -0.16$. Vector Lorentz-violating interactions, such as the b_μ coefficient, can contribute to the first harmonic signal, however within the Schmidt nuclear model for ^{21}Ne with a valence neutron such an interaction has already been excluded with sufficient precision by our previous experiment with ^3He [17]. The results of the daily fits for the c coefficients are shown in Fig. 4 for our data spanning a period of 3 months and the final results are summarized in Table 1. The systematic uncertainty is determined by the scatter of several analysis procedures, including fits of data without removal of long-term correlations and varying data cuts.

To convert our measurements from magnetic field units, we need an estimate of the nuclear operator $\langle I, I | \mathcal{P}_0^2 | I, I \rangle = \langle I, I | 2p_z^2 - p_x^2 - p_y^2 | I, I \rangle / \sqrt{6}$. Within the Schmidt model, ^{21}Ne has a valence neutron in the $d_{3/2}$ state. This gives $\langle I, I | \mathcal{P}_0^2 | I, I \rangle = -\sqrt{2/3} \langle p^2 \rangle / 5 = -\sqrt{8/3} m E_k / 5$ and we take the kinetic energy of the valence nucleon $E_k \sim 5$ MeV [9]. ^{21}Ne is better described

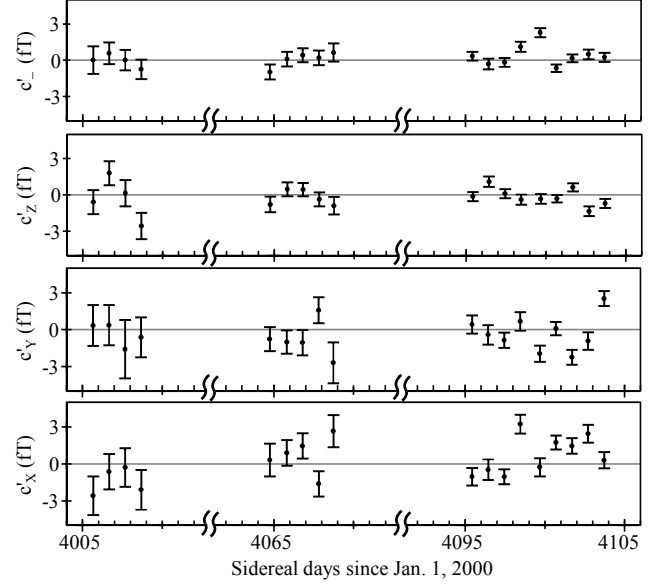


FIG. 4: Daily fits for the c coefficients defined in Eq. (6). The final statistical uncertainty is increased to account for reduced $\chi^2 = 2$ to 4.

by a collective wavefunction within the sd shell model and it should be possible to calculate the nuclear operator more precisely [28].

To evaluate the relative sensitivity of the comagnetometer to H_B and H_Q , we model the equilibrium spin density matrix of ^{21}Ne . Two processes dominate the spin evolution of ^{21}Ne , binary spin-exchange collisions with Rb [29] and spin-relaxation due to the interaction of its nuclear electric quadrupole moment with electric field gradients during binary atomic collisions [30]. At low Rb density, we measured ^{21}Ne spin relaxation time constant $T_Q = 87 \pm 4$ min, close to the relaxation rate of 103 ± 6 min that is predicted for our ^{21}Ne density from previous measurements of the ^{21}Ne nuclear quadrupole relaxation rate [18]. At normal operating temperature, the ^{21}Ne spin time constant was equal to 63 ± 2 min, implying an additional Rb- ^{21}Ne spin-exchange time constant $T_{ex} = 230 \pm 40$ min. This is reasonably consistent with Rb- ^{21}Ne spin-exchange time constant of 370 ± 70 min calculated from a previously measured Rb- ^{21}Ne spin-exchange rate constant [18]. The equilibrium ^{21}Ne polarization of 17% is also consistent with measured Rb polarization and spin-exchange and relaxation rates. In the density matrix model for the comagnetometer, we find the ratio of the signals produced by H_B and H_Q ,

$$\frac{S(Q)}{S(B_y)} = \frac{Q \langle I_z \rangle}{2\mu_{\text{Ne}} B_y / I} f(T_{ex}/T_Q) \quad (7)$$

where the function $f(T_{ex}/T_Q)$ ranges from $f(0) = 1$ to $f(\infty) = 3/2$ as the population distribution among the four spin states of ^{21}Ne changes depending on the nature of the dominant spin relaxation mechanism. For our operating parameters $f(2.6 \pm 0.4) = 1.27 \pm 0.03$. The

	North-South (fT)	East-West (fT)	Combined (fT)	Scaled ($\times 10^{-29}$)
$c_X = c_{YZ}^n + c_{ZY}^n$	$-0.90 \pm 1.8 \pm 2.3$	$0.75 \pm 0.39 \pm 0.50$	0.67 ± 0.62	4.8 ± 4.4
$c_Y = c_{XZ}^n + c_{ZX}^n$	$0.66 \pm 1.3 \pm 2.5$	$-0.42 \pm 0.36 \pm 0.33$	-0.39 ± 0.48	-2.8 ± 3.4
$c_Z = c_{XY}^n + c_{YX}^n$	$0.01 \pm 0.34 \pm 0.27$	$-0.23 \pm 0.19 \pm 0.13$	-0.17 ± 0.20	-1.2 ± 1.4
$c_- = c_{XX}^n - c_{YY}^n$	$0.65 \pm 0.34 \pm 0.32$	$0.04 \pm 0.19 \pm 0.20$	0.20 ± 0.24	1.4 ± 1.7

TABLE I: Results for the neutron c_{jk}^n coefficients measured in ^{21}Ne .

conversion factor to dimensionless c coefficients is

$$c = -c' \frac{10\mu_n}{3P_{Ne}fE_k} = 7.1 \times 10^{-29} \quad (8)$$

and our results for the neutron c_{jk}^n are given in the last column of Table 1.

We place limits on 4 of 5 spatial components of the neutron c coefficients that are 2 to 4 orders of magnitude more stringent than previous limits set with similar experiments using ^{21}Ne [5] and ^{201}Hg [4] spins, that had an energy resolution of $0.5 \mu\text{Hz}$. Our limits are also 4 orders of magnitude more stringent than limits on similar proton c coefficients set using ^{133}Cs atomic fountain clock [31] and many orders of magnitude more sensitive than limits for electron c coefficients [20]. Among astrophysical tests, the most stringent limits have been set on c_{0j} for neutrinos by Icecube at 10^{-27} and on c_{00} for protons at 10^{-23} from analysis of the spectrum of ultra-high energy cosmic rays. If we assume that Lorentz violation

is manifested by a difference between space and time in a preferred frame corresponding to the rest frame of the Cosmic Microwave Background, then our measurements of the spatial components c_{ij} in a frame moving with velocity of $10^{-3}c$ relative to the preferred frame have comparable sensitivities to the astrophysical measurements of c_{0j} and c_{00} .

This measurement represents the first experimental result using the ^{21}Ne -Rb-K comagnetometer. Our energy sensitivity is similar to the previous K- ^3He Lorentz-violation experiment [17] with a factor of 8 shorter integration time and without full optimization of the apparatus. The shot-noise sensitivity of the comagnetometer is already more than an order of magnitude better than the best results obtained with K- ^3He [32], allowing for future improvements in the vector and tensor Lorentz violation tests as well as other precision measurements. This work was supported by NSF Grant No. PHY-0969862.

-
- [1] V. W. Hughes, H. G. Robinson, and V. Beltran-Lopez, Phys. Rev. Lett. **4**, 342 (1960).
 - [2] R. W. P. Drever, Phil. Magazine, **6** 683 (1961).
 - [3] J. D. Prestage, J. J. Bollinger, Wayne M. Itano, and D. J. Wineland, Phys. Rev. Lett. **54**, 2387 (1985).
 - [4] S. K. Lamoreaux, J. P. Jacobs, B. R. Heckel, F. J. Raab, and E. N. Fortson, Phys. Rev. Lett. **57**, 3125 (1986).
 - [5] T. E. Chupp *et al.*, Phys. Rev. Lett. **63**, 1541 (1989).
 - [6] A.P. Lightman and D.L. Lee, Phys. Rev. D, **8**, 364, (1973).
 - [7] C.M. Will, Living Rev. Rel. **9**, 3 (2006).
 - [8] D. Colladay and V. A. Kostelecký, Phys. Rev. D **58**, 116002 (1998).
 - [9] V. A. Kostelecký and C. D. Lane, Phys. Rev. D **60**, 116010 (1999).
 - [10] S. Coleman and S. L. Glashow, Phys. Rev. D **59**, 116008 (1999).
 - [11] B. Altschul, Phys. Rev. Lett. **96**, 201101 (2006).
 - [12] B. Altschul, Phys. Rev. D **78**, 085018 (2008).
 - [13] F. W. Stecker and S. T. Scully, New J. Phys. **11**, 085003 (2009).
 - [14] P. Hořava, Phys. Rev. D **79**, 084008 (2009).
 - [15] D. Mattingly, Proc. of Science (QG-Ph) 026, (2008); arXiv:0802.1561v1.
 - [16] P. A. Bolokhov, S. Groot Nibbelink, and M. Pospelov, Phys. Rev. D **72**, 015013 (2005).
 - [17] J. M. Brown, S. J. Smullin, T. W. Kornack, and M. V. Romalis, Phys. Rev. Lett. **105**, 151604 (2010).
 - [18] R. K. Ghosh and M. V. Romalis, Phys. Rev. A **81**, 043415 (2010).
 - [19] M. V. Romalis, Phys. Rev. Lett. **105**, 243001 (2010).
 - [20] V. A. Kostelecký, N. Russell, Rev. Mod. Phys. **83**, 11 (2011).
 - [21] R. Abbasi *et al.*, Phys. Rev. D **82**, 112003 (2010).
 - [22] X.-J. Bi, Z. Cao, Y. Li, and Q. Yuan, Phys. Rev. D **79**, 083015 (2009).
 - [23] T. W. Kornack and M. V. Romalis, Phys. Rev. Lett **89**, 253002 (2002).
 - [24] T. W. Kornack, R. K. Ghosh and M. V. Romalis, Phys. Rev. Lett. **95**, 230801 (2005).
 - [25] T.W. Kornack, PhD Dissertation, Princeton University (2005).
 - [26] M. D. Rotondaro and G. P. Perram, J. Quan. Spec. Rad. Tran. **57**, 497 (1997).
 - [27] S. R. Schaefer, G. D. Cates, T.-R. Chien, D. Gonatas, W. Happer, and T. G. Walker, Phys. Rev. A **39**, 5613 (1989).
 - [28] W. Geithner *et al.*, Phys. Rev. C **71**, 064319 (2005).
 - [29] W. Happer *et al.*, Phys. Rev. A **29**, 3092 (1984).
 - [30] C. Cohen-Tannoudji, J. de Phys. **24**, 653 (1963).
 - [31] P. Wolf, F. Chapelet, S. Bize, and A. Clairon, Phys. Rev. Lett. **96**, 060801 (2006).
 - [32] G. Vasilakis, J. M. Brown, T. W. Kornack, and M. V. Romalis, Phys. Rev. Lett. **103**, 261801 (2009).